The Journal of Immunology

Histidine-Rich Glycoprotein Stimulates Human Neutrophil Phagocytosis and Prolongs Survival through CLEC1A

Yohei Takahashi, Hidenori Wake, Masakiyo Sakaguchi, Yukinori Yoshii, Kiyoshi Teshigawara, Dengli Wang and Masahiro Nishibori

J Immunol 2021; 206:737-750; Prepublished online 15 January 2021;
doi: 10.4049/jimmunol.2000817
http://www.jimmunol.org/content/206/4/737

The Journal of Immunology is published twice each month by
The American Association of Immunologists, Inc.,
1451 Rockville Pike, Suite 650, Rockville, MD 20852

Print ISSN: 0022-1767 Online ISSN: 1550-6606.

Histidine-Rich Glycoprotein Stimulates Human Neutrophil Phagocytosis and Prolongs Survival through CLEC1A

Yohei Takahashi,* Hidenori Wake,* Masakiyo Sakaguchi,† Yukinori Yoshii,* Kiyoshi Teshigawara,* Dengli Wang,* and Masahiro Nishibori*

Histidine-rich glycoprotein (HRG) is a multifunctional plasma protein and maintains the homeostasis of blood cells and vascular endothelial cells. In the current study, we demonstrate that HRG and recombinant HRG concentration dependently induced the phagocytic activity of isolated human neutrophils against fluorescence-labeled *Escherichia coli* and *Staphylococcus aureus* through the stimulation of CLEC1A receptors, maintaining their spherical round shape. The phagocytosis-inducing effects of HRG were inhibited by a specific anti-HRG Ab and enhanced by opsonization of bacteria with diluted serum. HRG and C5a prolonged the survival time of isolated human neutrophils, in association with a reduction in the spontaneous production of extracellular ROS. In contrast, HRG maintained the responsiveness of neutrophils to TNF-α, zymosan, and *E. coli* with regard to reactive oxygen species production. The blocking Ab for CLEC1A and recombinant CLEC1A-Fc fusion protein significantly inhibited the HRG-induced neutrophil rounding, phagocytic activity, and prolongation of survival time, suggesting the involvement of the CLEC1A receptor in the action of HRG on human neutrophils. These results as a whole indicated that HRG facilitated the clearance of *E. coli* and *S. aureus* by maintaining the neutrophil morphology and phagocytosis, contributing to the antiseptic effects of HRG in vivo. *The Journal of Immunology*, 2021, 206: 737–750.

Neutrophils are the most abundant leukocytes in systemic circulation (60–70%) and are present in the blood of healthy human adults at 2.5–7.5 × 10^9 cells per liter (1). Circulating neutrophils are maintained in a quiescent state until they are activated by signals such as inflammatory cytokines, activated complements, and bacterial peptides. Once neutrophils are activated, they interact with vascular endothelial cells and migrate to the inflamed site beyond the vascular endothelial cells. The neutrophils play a central role in the host defense against bacterial infection. The neutrophils are the main phagocytes in the front line and are responsible for the release of appropriate reactive oxygen species (ROS) and proteolytic enzymes as a defense against invading bacteria. Neutrophil extracellular trap (NET) formation may be another mode of defense by which neutrophils protect against the diffusion of bacteria, contributing to the host defense against bacterial infections. Indeed, patients with neutropenic or neutrophil adhesion deficiency have an increased risk of bacterial infection (2). In contrast, excessive ROS and NET release from neutrophils can be a major cause of tissue damage in many inflammatory diseases (3). Especially under septic conditions, the dysregulated neutrophils caused by infection are known to induce excessive ROS production, NET release, and aberrant neutrophil-vascular endothelial cell adhesion, which in turn trigger immunothrombus formation and failure in microcirculation, leading to disseminated intravascular coagulation and multiple organ failure (4, 5).

Histidine-rich glycoprotein (HRG) is a 75-kDa glycoprotein characterized by the existence of histidine-containing repeats (6). HRG consists of four domains: cystatin-like domain 1, cystatin-like domain 2, a histidine-rich region that contains 12 GHHPH sequences, and a C-terminal domain (7, 8). HRG was first isolated from human serum in 1972 and has since been found to be present in many vertebrates and aquatic invertebrates (8). In humans, HRG is synthesized by the liver parenchymal cells and is constitutively present in plasma at a concentration of 60–150 μg/ml (0.8–2.0 μM) (6, 7, 9). HRG has been detected on the cell surface of macrophages and monocytes (10) and in α granules of platelets and megakaryocytes (11). HRG has been reported to bind to various components, such as heparin (6), heparan sulfate (12), fibrin, fibrinogen (13), plasminogen (14), thrombospondin (15), complement complements (16), FcγRI (17, 18), FcγRII (19), IgG (20), zinc (21), and heme (22). Based on its binding profile, HRG has been suggested to play important roles in antifungal and antibacterial defense, the clearance of apoptotic and necrotic cells, and the regulation of coagulation/fibrinolysis (17, 23–27). In a previous

*Department of Pharmacology, Okayama University Graduate School of Medicine, Dentistry and Pharmaceutical Sciences, Okayama 700-8558, Japan; and †Department of Cell Biology, Okayama University Graduate School of Medicine, Dentistry and Pharmaceutical Sciences, Okayama 700-8558, Japan

ORCIDs: 0000-0002-2584-5005 (Y.T.); 0000-0002-0160-7379 (H.W.); 0000-0002-6048-2756 (K.T.); 0000-0002-0380-494X (D.W.).

Received for publication July 15, 2020. Accepted for publication November 20, 2020.

This work was supported by the Japan Agency for Medical Research and Development (JP19im0210109) and the Japan Society for the Promotion of Science (17K15580).

Y.T., M.S., D.W., and Y.Y. performed the experiments; Y.T., H.W., K.T., D.W., and M.N. analyzed the results and made the figures; H.W. and M.N. designed the research and critically revised the article; and Y.T. and M.N. designed the research and wrote the paper.

Address correspondence and reprint requests to Dr. Masahiro Nishibori, Department of Pharmacology, Okayama University Graduate School of Medicine, Dentistry and Pharmaceutical Sciences, 2-5-1, Shikata-cho, Okayama 700-8558, Japan. E-mail address: mbori@md.okayama-u.ac.jp

The online version of this article contains supplemental material.

Abbreviations used in this article: CHO, Chinese hamster ovary; CLEC1A, C-type lectin receptor 1A; CLEC1B, C-type lectin receptor 1B; CLP, cecal ligation puncture; HRG, histidine-rich glycoprotein; HSA, albumin from human serum; NET, neutrophil extracellular trap; PMN, polymorphonuclear cell; rCLEC1A-Fc, recombinant CLEC1A-Fc; rHRG, recombinant HRG; ROS, reactive oxygen species; wt, wild type.

study, we demonstrated that plasma HRG levels decreased significantly in a cecal ligation puncture (CLP) sepsis model in mice (28). In addition, we reported that supplementary treatment with HRG prevented high mortality in the CLP mice, in association with suppression of the tight adhesion and aggregation of neutrophils and platelets to the vascular endothelial cells. Moreover, it was shown in vitro that HRG maintained the spherical shape of human neutrophils with few microvilli on their surfaces as well as the reduced ROS production and easy passage of microcapillary vessels. Thus, the morphological and functional features induced by HRG may imply the neutrophil state keeping the quiescence and preventing from unnecessary activation. Phagocytosis of bacteria by neutrophils constitutes the frontline against infection. Therefore, it is very important to know whether the neutrophils with suppressed spontaneous ROS production by HRG respond properly to bacteria as primary phagocytic defense cells.

C-type lectins are a family of soluble and transmembrane receptors that bind carbohydrates via a carbohydrate-recognition domain. C-type lectin-like receptors (CTLRs) are a family of protein receptors involved in the recognition of self- and non–self-ligands and recognize not only carbohydrate ligands but also additional ligands such as proteins and lipids (29). With regard to their function, CTLRs have been reported to play many roles, including the uptake of microorganisms, clearance of apoptotic cells, modulation of immune responses through cytokine and chemokine, and regulation of cell–cell adhesion (30, 31). One of the orphan receptors, C-type lectin receptor 1A (CLEC1A), is a group V type II transmembrane receptor of the C-type lectin superfamily and is expressed by endothelial cells, dendritic cells, monocytes, and neutrophils in humans (32). Concerning the function of CLEC1A, two roles have been suggested: upregulation of TGF-β and activation of $CD4^+$ Th17 (33, 34). However, corresponding exogenous and endogenous ligands are unknown, and the downstream signaling remains uncharacterized. Recently, we identified CLEC1A as a novel receptor for HRG by using the HEK293T expression system and coimmunoprecipitation with the tethered ligand HRG (35).

In the current study, we evaluated the functional regulation of human neutrophils by native and recombinant HRG (rHRG), with a particular focus on bacterial phagocytosis and the involvement of CLEC1A receptors in the action of HRG. Because the life span of neutrophils has been speculated to be 24 h in the circulation, the effects of HRG on the longevity of neutrophils were also determined.

Materials and Methods

Reagent

HBSS was obtained from Life Technologies (Carlsbad, CA). Heparin was obtained from Mochida Pharmaceutical (Tokyo, Japan). Hoechst 33342, Calcein-AM, CM-H2DCFDA, pHrodo Red *Escherichia coli* BioParticles and pHrodo Red *Staphylococcus aureus* BioParticles were obtained from Thermo Fisher Scientific (Waltham, MA). fMLP was obtained from Peptide Institute (Minoh, Japan). Polymorphprep was obtained from AXIS-SHIELD (Oslo, Norway). Nickel-nitriloacetic acid (Ni-NTA) agarose was obtained from QIAGEN (Venlo, Netherlands). The ApoTox-Glo Triplex Assay kit was obtained from Promega (Madison, WI). C5a, IL-8, anti-human CLEC1A polyclonal Ab (AF1704), anti-human C-type lectin receptor 1B (CLEC1B) polyclonal Ab (AF1718), anti-human CLEC1A mAb (MAB1704), anti-human CLEC1B mAb (MAB1718), IgG goat control (AB-108-C), IgG2b mouse monoclonal isotype control (MAB004), and mouse monoclonal anti-phospho-tyrosine HRP-conjugated Ab were obtained from R&D Systems (Minneapolis, MN). Dulbecco PBS, albumin from human serum (HSA), albumin from BSA, LPS (*E. coli* 0111: B4), zymosan A from saccharomyces, isoluminol and HRP type IV (HRP) were obtained from Sigma-Aldrich (St. Louis, MO). Anti-human HRG mAb (rat IgG2a: no. 75–14), anti-human HRG mAb (rat IgG2b: no. 29–14), anti-human HRG polyclonal Ab (rabbit), and the control Abs corresponding to each were made in our laboratory.

Cell preparation

In accordance with the ethics approval and guidelines of Okayama University, blood was collected from healthy volunteers ($n = 3$) after obtaining informed consent. The blood was drawn from the cubital vein using heparin (10 U/ml) as anticoagulant. The polymorphonuclear cell (PMN) fraction was fractionated from human blood samples by density-gradient centrifugation. In detail, 5.0 ml of anticoagulated whole blood layered on 5.0 ml of polymorphprep in a 15-ml centrifuge tube was centrifuged at $500 \times g$ for 30 min at 22°C. After centrifugation, the PMNs band was harvested in a tube. The PMNs recovered were washed twice with PBS and were resuspended in HBSS to give an appropriate concentration for each experiment. All procedures were performed in the safety cabinet, and all instruments were sterilized. The solutions used were at least of a guaranteed reagent grade. The neutrophil fraction was 95% or more of total PMNs.

Cell lines

HEK293T (a human embryonic kidney cell line stably expressing the SV40 large T Ag; RIKEN BioResource Center, Tsukuba, Japan) were cultivated in D/F Medium (Thermo Fisher Scientific) supplemented with 10% FBS.

Stable transformants

The HEK293T cell–originated clones, HEK293T-CLEC1A (wild type [wt]) or HEK293T-CLEC1A (Δcyt; a deletion variant of the N-terminal cytoplasmic region [45 aa] of CLEC1A), which permanently express CLEC1A (wt) or CLEC1A (Δcyt) protein, were established by a convenient electroporation gene delivery method using our original plasmid, pSAKA-4B vector (36–38) and subsequent selection with puromycin at 20 μg/ml.

Purification of HRG from human plasma HRG and rHRG from HRG-expressing Chinese hamster ovary cells

HRG was purified from human plasma (supplied by the Japanese Red Cross Society) as previously described (28, 39). rHRG was obtained from Chinese hamster ovary (CHO) cells that were transfected with a human HRG expression vector. In brief, human HRG expression vector–transfected CHO cells were cultured with DMEM/Nutrient Mixture F-12 + 10% FCS + puromycin. The cell culture supernatant was incubated with Ni-NTA agarose gel for 2 h at 4°C. The gel was packed into a column and washed with 30 mM imidazole in PBS (−) (pH 7.4), then with 1 M NaCl + 10 mM PB (pH 7.4), and finally with PBS (pH 7.4). rHRG was eluted by 500 mM imidazole in PBS (−) (pH 7.4). Purified rHRG was identified by SDS-PAGE and Western blotting with a human HRG-specific Ab.

Neutrophil shape assay

Purified neutrophils were stained by Hoechst 33342 (Nuclei) and Calcein-AM (Cytosol) as described previously (28). The cell suspension was mixed with one of the reagents (BSA, HSA, fMLP, C5a, and HRG) and then aliquoted into a 96-well plate (BD Biosciences) (final cell concentration 5×10^4 cells per well). After incubation for 60 min at 37°C and 5% CO_2, scanning and analysis of neutrophil shape were performed using an IN Cell Analyzer 2000 (GE Healthcare) and IN Cell Analyzer Workstation software (GE Healthcare). Cell rounding (the average of maximum diameter/minimum diameter per cell) and cell area (μm^2/cell) were used as parameters to evaluate neutrophil shape.

Preparation of pHrodo E. coli *and* S. aureus

We used the pH-sensitive dye pHrodo *E. coli* and *S. aureus* reagents to evaluate the neutrophil phagocytic activity. PHrodo has weak fluorescence in a neutral or alkaline environment and has increased fluorescence intensity in an acidic environment such as in lysosomes. Using these reagents, we were able to measure phagocytic activity without separating neutrophils and free bacteria. The pHrodo *E. coli* and *S. aureus* reagents were dissolved in HBSS (0.5 mg/ml) and then sonicated for 5 min. After sonication, they were centrifuged at $200 \times g$ for 5 min. The supernatants were used for phagocytosis assay. Opsonization of the pHrodo *E. coli* and *S. aureus* reagents was performed using 20% human serum. The pHrodo *E. coli* and *S. aureus* reagents were dissolved in 2 ml of 5-fold diluted human serum and incubated for 15 min at 37°C and 5% CO_2. After washing the reagents twice and adjusting their concentration to 0.5 mg/ml

by HBSS, we used them for the phagocytosis assay. Unopsonized pHrodo was incubated with HBSS instead of serum.

Neutrophil phagocytosis assay

Purified neutrophils were stained by Hoechst 33342 and Calcein-AM. The cell suspension was mixed with one of the reagents (BSA, HSA, fMLP, C5a, or HRG) and then aliquoted into a 96-well plate. After incubation for 30 min at 37˚C and 5% CO_2, the pHrodo *E. coli*, pHrodo *S. aureus*, or zymosan A was added to the well (final cell concentration: 5×10^4 cells per well; final pHrodo concentration: 25 μg/well). After incubation for 60 min (*E. coli*) or 120 min (*S. aureus* and zymosan A) at 37˚C and 5% CO_2, scanning and analysis of neutrophil phagocytosis were performed using an IN Cell Analyzer 2000 and IN Cell Analyzer Workstation software. Total pHrodo fluorescence areas were measured, and the average area of pHrodo per cell (μm^2/cell) was used to evaluate the amount of neutrophil phagocytosis.

Neutrophil viability assay

Purified neutrophils were stained by Hoechst 33342 and Calcein-AM. The neutrophil suspension was aliquoted to a 96-well plate in a volume of 100 μl (final cell concentration 5×10^4 cells per well) with one of the reagents (HSA, fMLP, C5a, HRG: final concentration 1 μM) in the presence or absence of Ab (rat IgG2a control Ab, rat anti-human HRG Ab [IgG2a]: final concentration 10 ng/ml). We scanned the neutrophils and counted the calcein-positive neutrophil number at 0, 1, 2, 4, 6, 9, 12, 18, and 24 h after stimulation at 37˚C and 5% CO_2 using an IN Cell Analyzer 2000. We evaluated the time-dependent change in neutrophil number.

ApoTox-Glo Triplex Assay

For neutrophil viability assays, we used an ApoTox-Glo Triplex Assay kit (Promega GmbH; High-Tech-Park, Mannheim, Germany). The neutrophil suspensions were treated with one of the reagents (HBSS, HSA, fMLP, C5a, HRG: 1.0 μM) and seeded into a 96-well plate. After incubation for 6 h at 37˚C and 5% CO_2, 20 μl of viability/cytotoxicity reagent containing both glycylphenylalanyl-aminofluorocoumarin and bis-alanylalanyl-phenylalanyl-rhodamine 110 substrate was added to each well, and then these ingredients were briefly mixed for 30 s and incubated for 30 min at 37˚C. Fluorescence was measured at 400ex/505em (viability) and 485ex/520em (cytotoxicity) using a FlexStation3 (Molecular Devices, San Jose, CA). Next, 100 μl of Caspase-Glo 3/7 reagent was added to each well, and the samples were mixed and then incubated at room temperature for 30 min. Luminescence was measured using the FlexStation3.

Detection of extracellular and intracellular ROS production in neutrophils

One of the reagents or a combination of two reagents (HSA, fMLP, C5a, HRG: 1 μM; rat IgG2a control Ab, rat anti-human HRG Ab [IgG2a]: 10 μg/ml; zymosan A from saccharomyces: 10 μg/ml; LPS and TNF-α: 50 ng/ml; autoclaved *E. coli* or *S. aureus*: 5×10^5 from 10^6) were aliquoted to a 96-well polystyrene plate in a volume of 50 μl. In the extracellular ROS production assay, the neutrophil suspension with isoluminol (final concentration: 50 μM) and HRP (final concentration: 4 U/ml) was aliquoted to each well in a volume of 50 μl (final concentration 5×10^4 cells). Neutrophil extracellular ROS production was measured every 5 min for 45 min, and then chemiluminescence intensity was evaluated at 30 min after the start of incubation at 37˚C by measurement using FlexStation3. In the intracellular ROS production assay, the neutrophil suspension with CM-H2DCFDA (final concentration, 10 μM) was aliquoted to each well in a volume of 50 μl (final concentration 5×10^4 cells). Neutrophil intracellular ROS production was measured as the fluorescence intensity (485ex/538em) at 60 min after the start of incubation at 37˚C using a FlexStation3.

Western blotting

The collected cell pellets were lysed with M-PER buffer (Thermo Fisher Scientific). The extracted cell specimens were then subjected to SDS-PAGE, and the electrophoresed gel was transferred to the polyvinylidene difluoride (PVDF) membrane. BSA was used for the membrane blocking. The detection of the phosphorylation modification on tyrosine and serine was performed by using mouse monoclonal anti-phospho-tyrosine HRP-conjugated Ab or mouse monoclonal anti-phospho-serine Ab (BD Biosciences Pharmingen, San Diego, CA) with the HRP-conjugated rabbit anti-mouse IgG Ab (Cell Signaling Technology, Danvers, MA).

Statistical analysis

Statistical analysis was determined using the unpaired Student *t* test for comparisons between two groups. For multiple comparisons, ANOVA followed by Dunnett test and Tukey test was used. All data are presented as means ± SEM. The p values < 0.05 were considered statistically significant.

Results

HRG induces spherical shape change of purified human neutrophils

We investigated the neutrophil morphology after the treatment with test reagents (BSA, HSA, fMLP, C5a, HRG, each at 1-μM concentration) for 60 min (Fig. 1A). The cell rounding and cell area were significantly reduced in the HRG-treated group compared with the other groups (Fig. 1B, 1C). Neutrophils treated with HRG and rHRG showed a decreased cell rounding and cell area in a concentration-dependent manner (Fig. 1D–F). We verified the specificity of the HRG effects on neutrophils by adding anti-HRG Ab (final concentration of Ab: 10 μg/ml; HRG: 0.25 μM) to the incubation media. Neutrophil rounding was suppressed by two kinds of anti-HRG mouse mAbs as well as rabbit polyclonal Ab (Fig. 1G–I). These blocking effects of Abs strongly indicated the specificity of the HRG effects on human neutrophils.

HRG stimulates the phagocytic activity of bacteria in vitro

Phagocytosis of bacteria and fungi is one of the main functions of neutrophils. To evaluate the effects of HRG on neutrophil phagocytic activity, we performed a phagocytosis assay using *E. coli* and *S. aureus* labeled by pHrodo red. pHrodo red is a pH-sensitive fluorescence probe and exhibits red fluorescence under acidic conditions such as those within phagosomes. For the quantitative measurements, we determined the pHrodo-derived red fluorescence area in the neutrophils (total area: μm^2/cell) as the phagocytic activity. pHrodo-derived red fluorescence of *E. coli* and *S. aureus* was observed in HRG- and rHRG-treated neutrophils but was not observed in HBSS- and HSA-treated neutrophils (Fig. 2A, 2B). In the videos, the enhanced movement of neutrophils was apparent after the addition of HRG to the suspensions (Supplemental Videos 1–4; conditions: total for 2.5 h, one flame represents 3 min). C5a (1 μM) treatment stimulated the phagocytosis of *E. coli* as well as *S. aureus* by neutrophils, whereas the same concentrations of fMLP and IL-8 as well as LPS (100 μg/ml) and TNF-α (10 ng/ml) did not show any stimulatory effects on bacterial phagocytosis (Fig. 2C, 2D). The concentration dependence of the effects of HRG and rHRG on *E. coli* and *S. aureus* is shown in Fig. 2E, 2F. The results showed that the effects were maximal at a concentration of 0.3 μM for both HRGs. The anti-HRG Ab (10 μg/ml) almost completely suppressed the effects of HRG on *E. coli* phagocytosis by neutrophils, whereas the same concentration of anti-HRG Ab only partially inhibited the effects of HRG on *S. aureus* phagocytosis (Fig. 2G–I).

HRG also stimulates the phagocytic activity of zymosan A and opsonized bacteria

To investigate whether HRG also promotes neutrophil phagocytosis of other bacteria, we performed a phagocytosis assay using zymosan A labeled by pHrodo red. As observed in the *E. coli* and *S. aureus* assays, zymosan A fluorescence was incorporated into HRG-treated neutrophils, whereas almost no fluorescence was detected in HBSS-, HSA-, or fMLP-treated neutrophils (Fig. 3A, 3B). Next, we investigated the effect of HRG on neutrophil phagocytosis in opsonized bacteria.

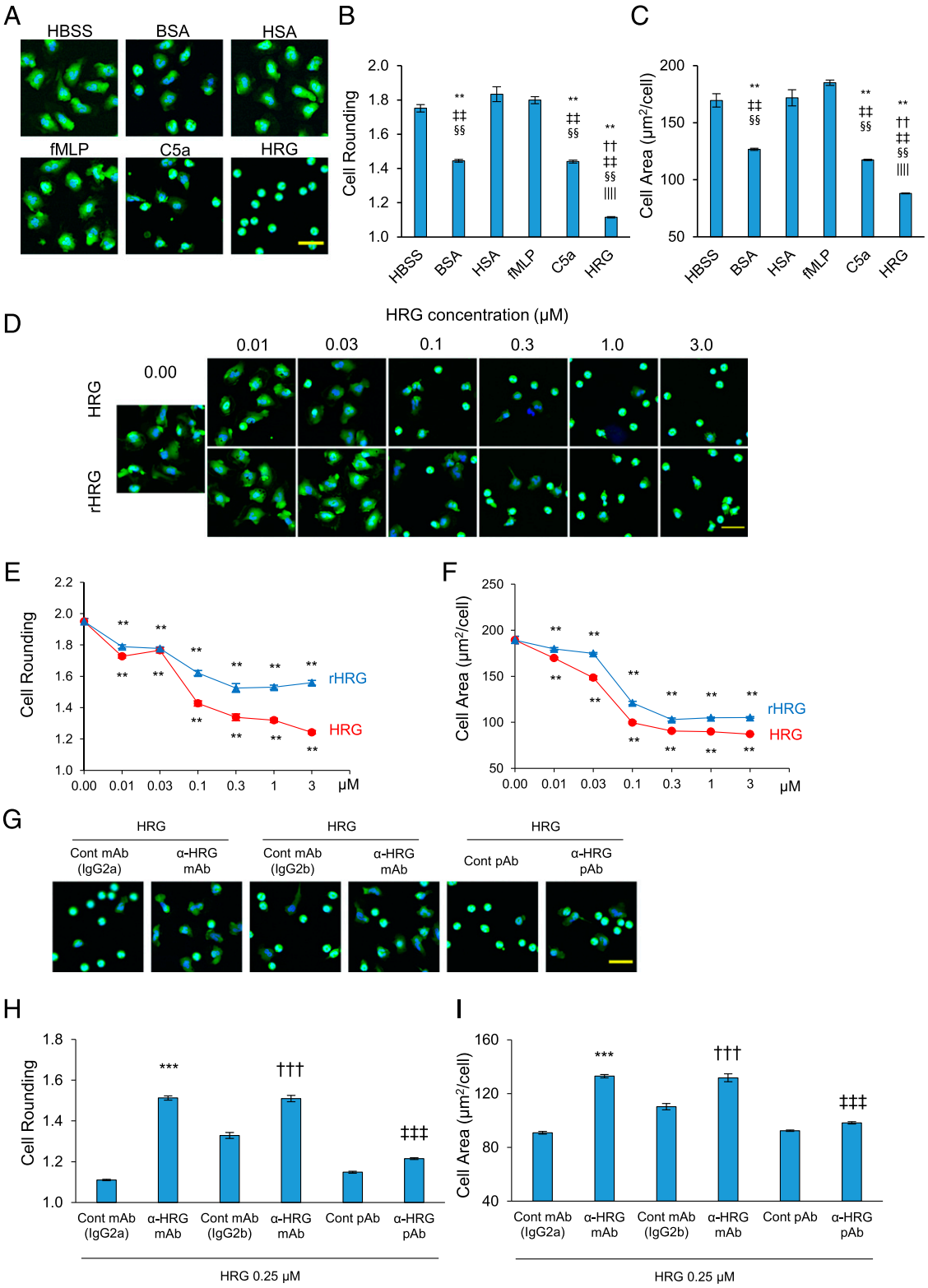

FIGURE 1. Effects of HRG and rHRG on the shape of purified human neutrophils. (**A**) The neutrophils were labeled with calcein-AM (cytosol, green) and Hoechst 33342 (nuclei, blue), and the cell shape was observed under a fluorescent microscope at 60 min after stimulation (BSA, HSA, fMLP, C5a, and HRG: 1 μM). Typical results from four independent experiments are shown. (**B** and **C**) Quantitative analysis of cell shape by cell rounding (average of maximum diameter/minimum diameter per cell) and cell area (μm^2/cell). $^{**}p < 0.01$ versus HBSS, $^{\dagger\dagger}p < 0.01$ versus BSA, $^{\ddagger\ddagger}p < 0.01$ versus HSA, $^{\S\S}p < 0.01$ versus fMLP, $^{||||}p < 0.01$ versus C5a. (**D**) Concentration-dependent effects of HRG and rHRG on neutrophil shape. Typical results from four independent experiments are shown. The neutrophils were incubated with different concentrations of HRG or rHRG for 60 min. (**E** and **F**) The concentration-response curves of the effects of HRG and rHRG. $^{**}p < 0.01$ versus HRG and rHRG: 0.00 μM. (**G**) Effects of different anti-HRG Abs (anti-human HRG mAb [rat IgG2a: no. 75–14] and anti-human HRG mAb [rat IgG2b: no. 29–14]) on the shape change-inducing effects of HRG (0.25 μM). (**H** and **I**) The cell rounding and cell area were determined as described above. $^{***}p < 0.001$ versus mouse IgG2a control, $^{\dagger\dagger\dagger}p < 0.001$ versus mouse IgG2b control, $^{\ddagger\ddagger\ddagger}p < 0.001$ versus rabbit IgG control. (A, D, and G) Original magnification ×20 and digital zoom ×64; scale bar, 25 μm. (B, C, E, F, H, and I) The results shown are the means ± SEM of 12 fields.

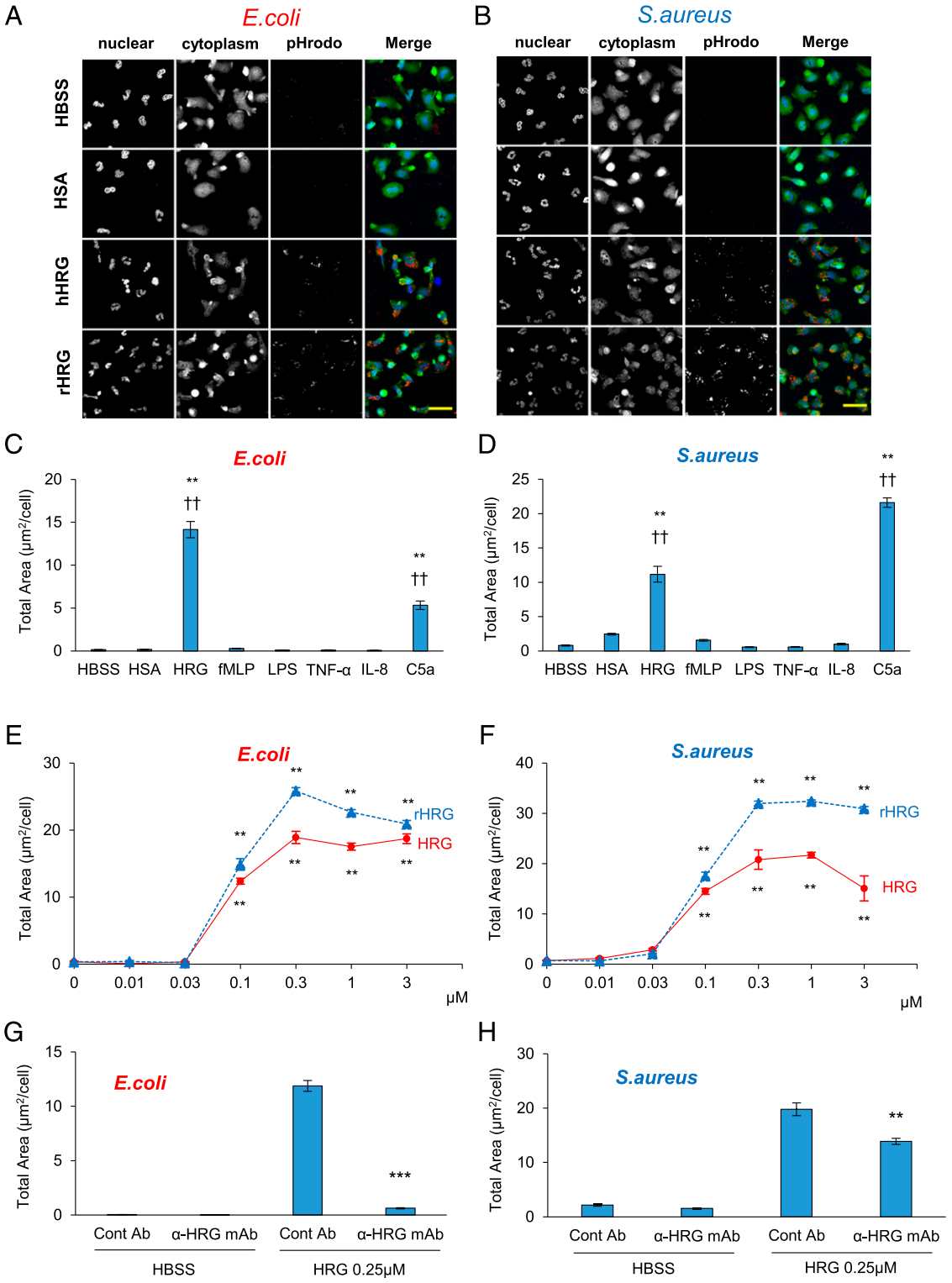

FIGURE 2. HRG stimulated phagocytic activity in neutrophils. (**A** and **B**) The neutrophils were labeled with calcein and Hoechst 33342. pHrodo *E. coli* (A) or *S. aureus* (B) (red) was added to neutrophils, and the phagocytosis proceeded for 60 min (*E. coli*) or 120 min (*S. aureus*) under different conditions (HSA, HRG, and rHRG: 1 μM). Original magnification ×20 and digital zoom ×64; scale bar, 25 μm. (**C** and **D**) Quantitative analysis of pHrodo *E. coli* and *S. aureus* by the total red fluorescent area (average area of pHrodo per cell: μm^2/cell) obtained under different conditions (BSA, HSA, fMLP, C5a, and HRG: 1 μM; LPS and TNF-α: 10 ng/ml; IL-8: 100 ng/ml). $^{**}p < 0.01$ versus HBSS, $^{\dagger\dagger}p < 0.01$ versus HSA. (**E** and **F**) The concentration-response curves for the effects of HRG and rHRG on phagocytosis in neutrophils $^{**}p < 0.01$ versus without HRG and rHRG. (**G** and **H**) Blocking of HRG-induced neutrophil phagocytosis by anti-HRG Ab (anti-human HRG mAb [rat IgG2a: no. 75–14]) and the corresponding control Ab (Ab: 10 μg/ml; HRG and rHRG: 0.25 μM). $^{**}p < 0.01$, $^{***}p < 0.001$ versus HRG + Cont Ab. (C–H) The results shown are the means ± SEM of 12 fields.

E. coli and *S. aureus* that were opsonized with 5-fold diluted serum were significantly phagocytosed by nontreated neutrophils (Fig. 3C). This trend was particularly remarkable in *S. aureus* (Fig. 3D, 3F). In HRG-treated neutrophils, the phagocytic activity of neutrophils was enhanced by opsonization of bacteria.

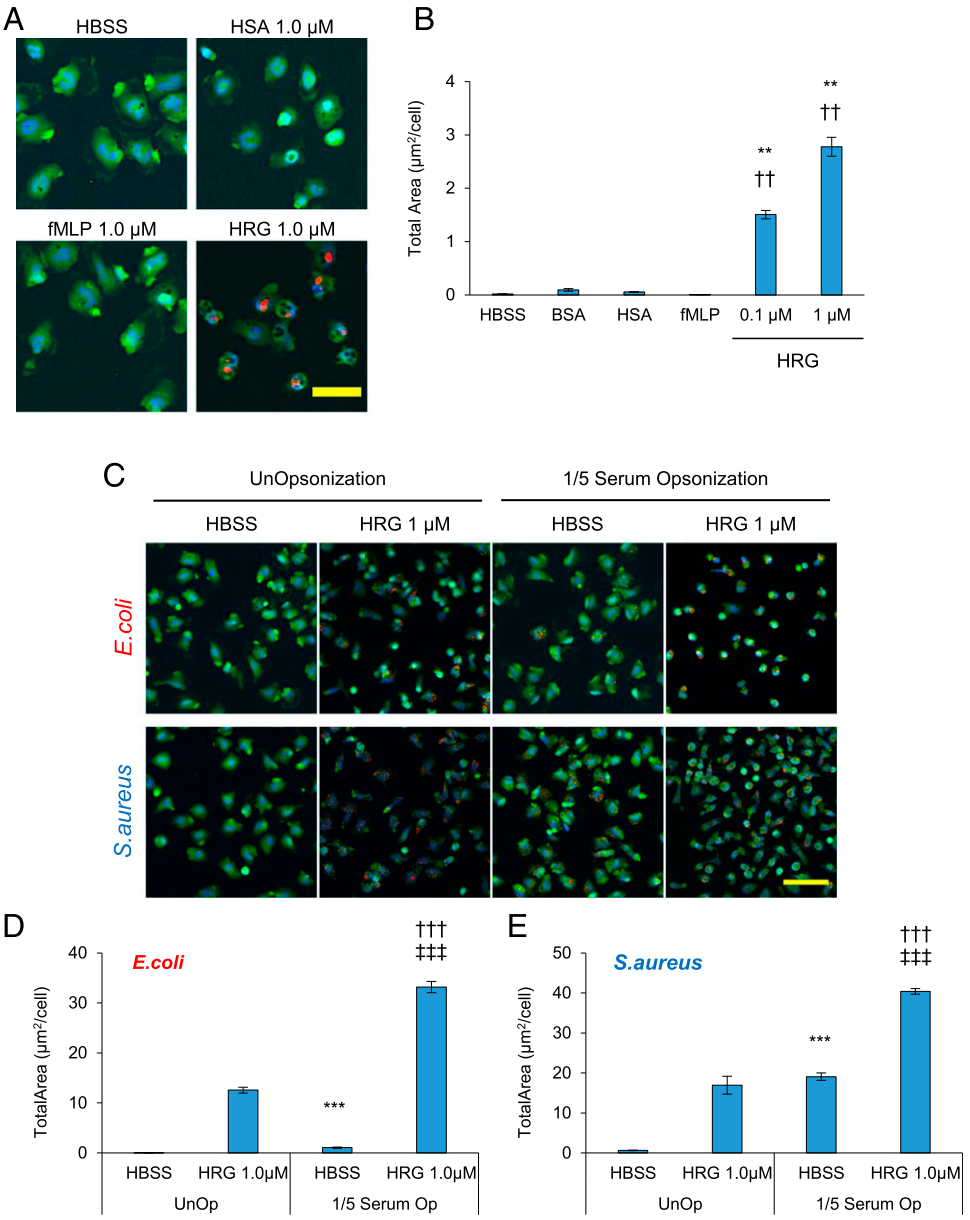

FIGURE 3. HRG stimulated phagocytotic activity of neutrophils against zymosan A and opsonized bacteria. (**A**) The neutrophils were labeled with calcein and Hoechst 33342. pHrodo zymosan A (red) was added to neutrophils, and the phagocytosis proceeded for 120 min under different conditions (HSA, fMLP, HRG, and rHRG: 1 μM). Original magnification ×20 and digital zoom ×64; scale bar, 25 μm. (**B**) Quantitative analysis of pHrodo zymosan A by the total red fluorescent area (average area of pHrodo per cell: μm^2/cell) obtained under different conditions (BSA, HSA, fMLP, C5a, and HRG: 0.1, 1 μM). $^{**}p < 0.01$ versus HBSS, $^{\dagger\dagger}p < 0.01$ versus HSA. (**C**) Neutrophil phagocytosis assay with opsonized-(1/5 serum) or unopsonized-pHrodo *E. coli* or *S. aureus*. Original magnification ×20 and digital zoom ×16; scale bar, 50 μm. (**D** and **E**) Quantitative analysis of opsonized- or unopsonized-pHrodo *E. coli* or *S. aureus* by the total red fluorescent area obtained under different conditions (without or with HRG 1 μM). $^{***}p < 0.001$ versus unopsonized HBSS, $^{\dagger\dagger\dagger}p < 0.001$ versus unopsonized HRG, $^{\ddagger\ddagger\ddagger}p < 0.001$ versus opsonized HBSS.

Effects of HRG on viability of human neutrophils

Because it is well known that neutrophils survive only a short time in the circulation, we determined the effects of HRG on neutrophil viability under different conditions, including in the presence and absence of HRG. Fig. 4A shows the surviving neutrophils with the cytosolic staining with calcein 6 and 12 h after the start of incubation. The number of surviving neutrophils decreased rapidly in the HBSS, fMLP (1 μM), and HSA (1 μM) groups (Fig. 4B). Compared with these three groups, the neutrophils treated with C5a (1 μM) and HRG (1 μM) exhibited a significantly prolonged survival time (Fig. 4B). When we determined the neutrophil viability in the presence of C5a or HRG at 12 h, more than 50% of neutrophils survived, whereas the neutrophil viability in the former three groups was close to null (Fig. 4C). The prolongation of survival time by HRG (0.1 μM) was blocked by the addition of anti-HRG mAb (Fig. 4D). The concentration dependence of the effects of HRG and rHRG is shown in Fig. 4E. The results showed that the effects were maximal at a concentration of 0.3 μM for both HRGs. To assess neutrophil viability from a different perspective, we measured live-cell protease activity in cells using an ApoTox-Glo Triplex Assay kit. This live-cell protease becomes inactive upon loss of cell membrane integrity and leaks into the surrounding culture medium. The results showed that HRG-treated neutrophils retained a higher level of protease activity compared with the other groups (Fig. 4G), suggesting the integrity of the cell membrane and viability of the cells.

Extracellular ROS production of neutrophils was reduced by HRG but responsive to stimulants

We measured the extracellular ROS production from neutrophils treated with each reagent (HBSS, HSA, fMLP, C5a, and HRG: 1 μM) at 30 min after reagent addition. The ROS production levels were significantly reduced in the C5a- and HRG-treated group compared with the other groups (Fig. 5A). The decrease in the amount of ROS production by HRG was antagonized by the addition of anti-HRG Ab (final concentration: 10 μg/ml; HRG: 0.25 μM) (Fig. 5B). The potencies of the HRG and rHRG effects on ROS production were almost the same (Fig. 5C). Next, we elucidated the influence of stimulants (zymosan A, LPS, or TNF-α) on the amount of ROS production from

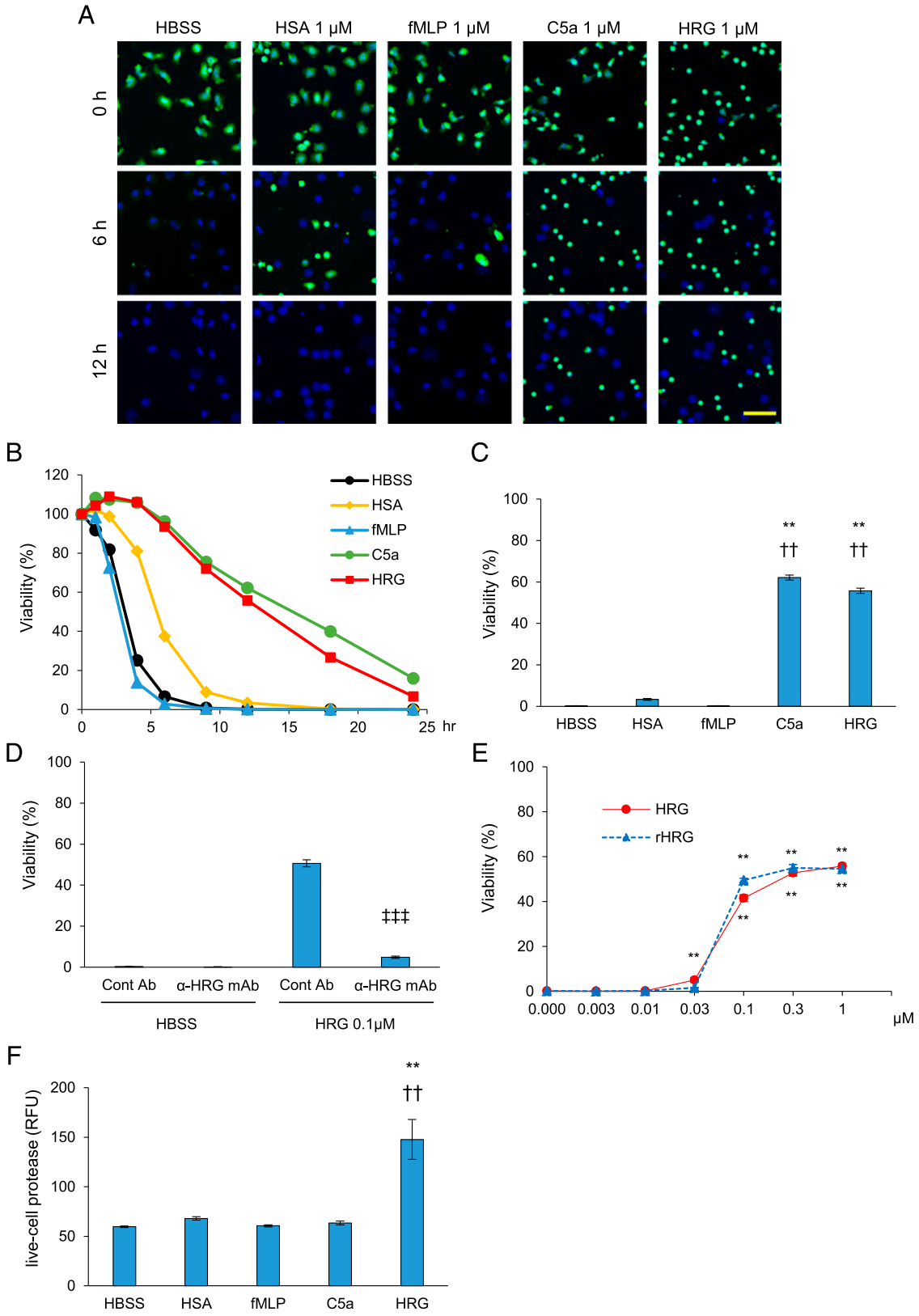

FIGURE 4. HRG and rHRG prolonged the survival time in purified human neutrophils. (**A**) The viability of neutrophils was determined under fluorescent microscopy by the retention of calcein in the cytosol (green) under different condition (HSA, fMLP, C5a, and HRG: 1 μM) at each time point (0, 6, and 12 h). The panel shows fluorescence microscopy images stained by Hoechst 33342 (blue) and calcein (green). Original magnification ×20 and digital zoom ×16; scale bar, 50 μm. (**B** and **C**) Viability of the neutrophils was calculated as a percentage of the initial number of calcein fluorescence-positive cells. (C) The graph represents the viability of each group at 12 h. $^{**}p < 0.01$ versus HBSS, $^{\dagger\dagger}p < 0.01$ versus HSA. (**D**) Blocking of the effects of HRG (0.1 μM) on neutrophil survival by anti-HRG Ab (anti-human HRG mAb [rat IgG2a: no. 75–14]) and the corresponding clone-matched control Ab (Ab: 10 μg/ml) at 12 h. $^{\ddagger\ddagger\ddagger}p < 0.001$ versus HRG + control IgG. (**E**) The concentration-response curves for the effects of HRG and rHRG on neutrophil survival at 12 h. $^{**}p < 0.01$ versus without HRG and rHRG. (**F**) Neutrophil viability was evaluated by live-cell protease activity using an ApoTox-Glo Triplex Assay kit at 6 h. The results shown are the means ± SEM of three wells. $^{**}p < 0.01$ versus HBSS, $^{\dagger\dagger}p < 0.01$ versus HSA. (B–F) The results shown are the means ± SEM of 12 fields.

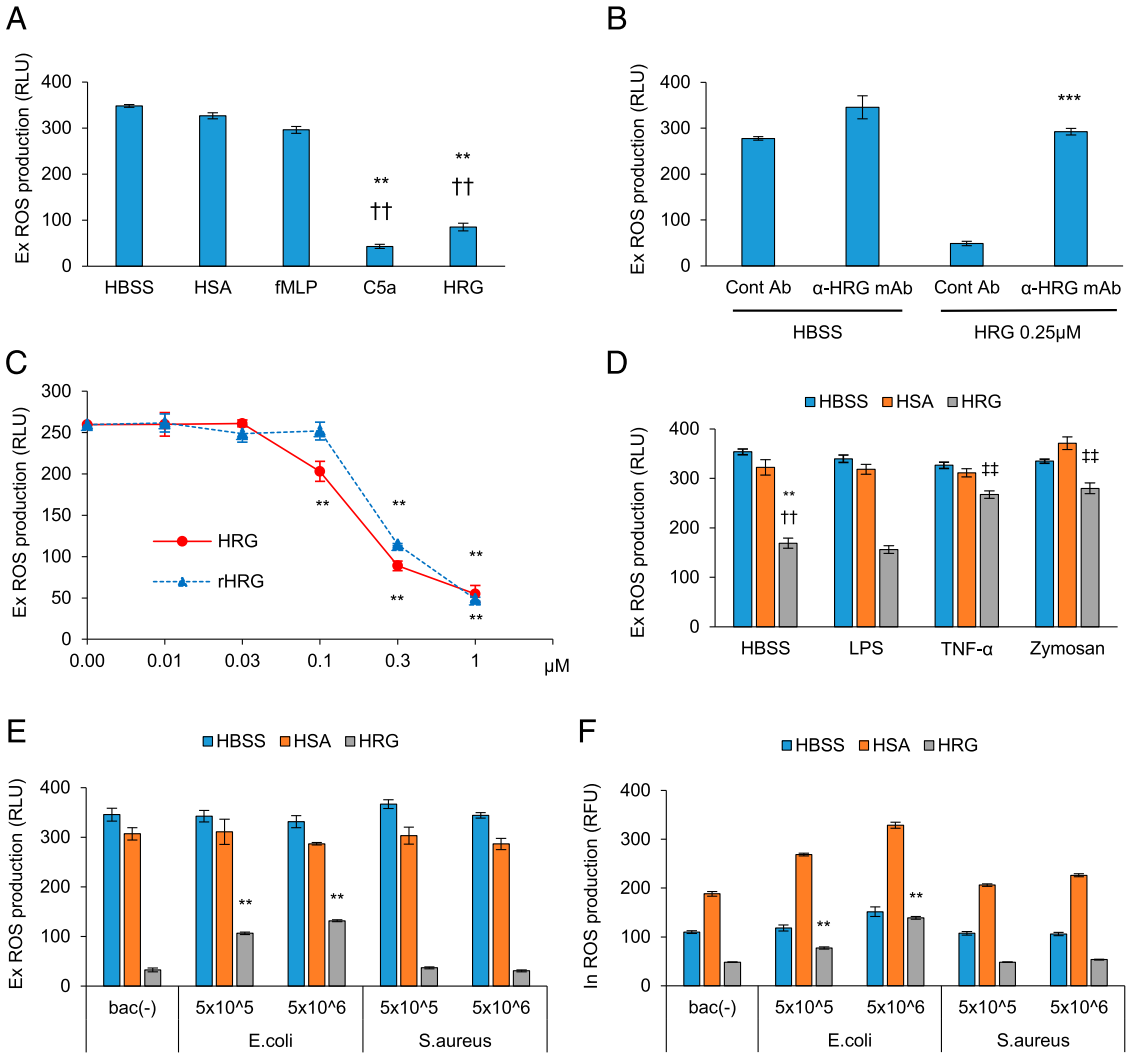

FIGURE 5. Neutrophils maintained in a quiescent state by HRG released the extracellular ROS by zymosan A, TNF-α, or autoclaved *E. coli* stimulation. (**A**) The neutrophils were incubated under different conditions (HSA, fMLP, C5a, and HRG: 1 μM), and the production of extracellular ROS was measured at 30 min. $^{**}p < 0.01$ versus HBSS, $^{\dagger\dagger}p < 0.01$ versus HSA. (**B**) Blocking of the HRG effects (0.25 μM) on neutrophil extracellular ROS production by anti-HRG Ab (anti-human HRG mAb [rat IgG2a: no. 75–14]) and the corresponding clone-matched control Ab (Ab: 10 μg/ml). Extracellular ROS was determined at 30 min. $^{***}p < 0.001$ versus HRG + Cont Ab. (**C**) The concentration-response curves for the effects of HRG and rHRG on the neutrophil extracellular ROS production assay. Extracellular ROS was determined at 30 min. $^{**}p < 0.01$ versus HRG and rHRG: 0.00 μM. (**D**) The neutrophils were stimulated with zymosan A from saccharomyces 10 μg/ml, LPS 50 ng/ml, or TNF-α 50 ng/ml in the presence of HSA 1.0 μM or HRG 1.0 μM. The extracellularly produced ROS was determined at 30 min. $^{**}p < 0.01$ versus HBSS + HBSS, $^{\dagger\dagger}p < 0.01$ versus HSA + HBSS, $^{\ddagger\ddagger}p < 0.01$ versus HRG + HBSS. (**E** and **F**) The neutrophils were incubated with a combination of reagents (HBSS, HSA: 1.0 μM; HRG: 1.0 μM) and autoclaved *E. coli* or *S. aureus* (final concentration: 5×10^5 or 5×10^6 per well) in the presence or absence of HRG 1 μM, and the levels of extracellularly and intracellularly produced ROS were determined at 30 min. $^{**}p < 0.01$ versus HRG + bacteria (-) [bac(-)]. (A–F) The results shown are the means ± SEM of three wells.

neutrophils in the presence or absence of HRG. In the absence of HRG, the levels of ROS production seemed to be maximal irrespective of the stimulants, and no change in ROS production was observed with the addition of LPS, TNF-α, or zymosan A. In contrast, in the presence of HRG, a stimulation-dependent increase in the amount of ROS production by zymosan A or TNF-α was observed (Fig. 5D). Next, we elucidated the influence of the autoclaved bacteria on the amount of ROS production from neutrophils in the presence or absence of HRG (1 μM). The ROS production levels in the HBSS and HSA groups were not changed by the addition of autoclaved *E. coli* and *S. aureus* (Fig. 5E). The ROS production levels in the presence of HRG increased with the addition of autoclaved *E. coli* but did not increase with the addition of autoclaved *S. aureus*. Intracellular ROS production was verified using an experimental system similar to that used for extracellular ROS production. The intracellular ROS production levels in HBSS did not change with the addition of autoclaved *E. coli* and *S. aureus* (Fig. 5F). In the HSA group, the ROS production levels increased compared with those in the HBSS group in the absence of bacteria. In the HRG group, the ROS production levels decreased compared with those in the HBSS group in the absence of bacteria. The ROS production levels in the HSA and HRG groups were increased with the addition of autoclaved *E. coli* but did not change with the addition of autoclaved *S. aureus*–like extracellular ROS production.

Effects of blocking Abs against CLEC1A and CLEC1B on the action of HRG on neutrophils

In our previous study, we identified CLEC1A as an HRG receptor (35). Also, CLEC1B may be involved in the action of HRG on NK cells (37). Therefore, we examined whether the blocking anti-CLEC1A or CLEC1B (goat polyclonal and mouse IgG2b

monoclonal) Abs would affect the shape changes, phagocytosis, survival, or suppression of extracellular ROS production induced by HRG (final concentration of Abs: 10 μg/ml; HRG: 0.25 μM). In the shape assay, CLEC1A polyclonal and mAbs inhibited the neutrophil morphology change induced by HRG (Fig. 6A). The form factor and cell area were significantly increased in the anti-CLEC1A Ab-treated groups compared with the control Ab-treated groups (Fig. 6B, 6C). In the phagocytosis assay, anti-CLEC1A polyclonal, CLEC1A monoclonal, and CLEC1B mAbs significantly inhibited the phagocytosis of *E. coli* and *S. aureus* (Fig. 6D, 6E). In the viability assay, only the CLEC1A polyclonal Ab partially antagonized the effect of HRG on the survival time of neutrophils (Fig. 6F). In the assay of extracellular ROS production, anti-CLEC1A and CLEC1B polyclonal Abs antagonized the effect of HRG (Fig. 6G).

Next, we examined whether the recombinant CLEC1A-Fc (rCLEC1A-Fc) fusion protein as a decoy molecule would inhibit the effect of HRG on neutrophils by binding to HRG in the incubation media. In the shape assay, treatment with the rCLEC1A-Fc fusion protein inhibited the rounding-inducing effects of HRG in a concentration-dependent manner (Fig. 7A–C). In the phagocytosis assay, the addition of the rCLEC1A-Fc fusion protein did not affect the phagocytosis in the absence of HRG but did reduce phagocytosis in both *E. coli* and *S. aureus* in the presence of HRG in a concentration-dependent manner (Fig. 7D, 7E). In the viability assay, the addition of the rCLEC1A-Fc fusion protein partially reduced the survival time–prolonging effect of HRG (Fig. 7F). In the extracellular ROS production assay, the decrease in the amount of ROS production by HRG was efficiently inhibited by the rCLEC1A-Fc fusion protein (Fig. 7G).

Detection of intracellular signals induced by HRG using CLEC1A-expressing HEK293T cells

To examine if certain signal transduction arises in the CLEC1A downstream upon HRG binding, we tried to conduct Western blotting for entire phospho-proteins, which will be upregulated in response to HRG stimulation, because phosphorylation modification is a general hallmark that couples with signal transduction. In fact, another CLEC family protein, CLEC1B, triggers its typical signal transduction with the promoted phosphorylation modification of several signal molecules one after another (Fig. 8A) (40). As shown in Fig. 8B, we found that one protein band of the tyrosine (Tyr)-based phosphorylation and five protein bands of serine (Ser)-based phosphorylation are pronouncedly upregulated in the HEK293T stable clone with CLEC1A (wt) overexpression when the clone was stimulated with HRG. In contrast, intriguingly, the phosphorylation level remarkably lowered in the CLEC1A- (Δcyt) (a deletion variant of cytoplasmic domain of CLEC1A) overexpressing cells in comparison with that of CLEC1A (wt) cells, which were observed in both cases of phospho-Tyr and phospho-Ser detections, and the lowered levels of the phosphorylation were not increased even under the presence of HRG in culture anymore. These results suggest that CLEC1A has its featured signal pathway(s) coupled with the phosphorylation modification and the downstream signal(s) in part are upregulated by the HRG-CLEC1A binding.

Discussion

Phagocytosis is a process by which cells engulf particles of more than 0.5 μm in size, including microbes and apoptotic cells. The initial elimination of invading bacteria from the body is performed by phagocytes. The neutrophils are the major phagocytes on the front line of innate immunity and play a key role in the host defense against bacterial infection. Phagocytosis of bacteria by neutrophils might involve several steps: the recognition of bacteria by receptor molecules on the surface of neutrophils, adhesion of neutrophils to bacteria, engulfment of bacteria into endophagosomes, and killing and digestion of bacteria inside the phagolysosomes. Although it is well known that the phagocytic processes are facilitated by the opsonization of bacteria by activated complements and the immune complex through Fc and complement receptors on neutrophils, there might exist a non-opsonized phagocytic process. In the current study, we clearly demonstrated that HRG alone can induce the phagocytic activity of neutrophils against fluorescence-labeled *E. coli* and *S. aureus*. The phagocytosis-inducing effects of HRG alone were enhanced by the addition of serum, suggesting the synergy of HRG effects with opsonization of bacteria.

We also showed that the phagocytosis-enhancing effects of HRG were associated with an increase in ROS production and prolongation of survival time. rHRG produced in CHO cells had a similar potency to native HRG purified from human plasma in terms of the capacities for inducing round neutrophils, prolonging survival, and enhancing phagocytosis. In addition, HRG retained the responsiveness of the neutrophils to two other proinflammatory factors, TNF-α and zymosan, with regard to ROS production. Collectively, these results indicate that HRG strongly activates bacterial phagocytosis in vitro.

Recently, Gao et al. identified a receptor for HRG, CLEC1A, using a tethered HRG ligand and candidate expression system in HEK293T cells (35). Using the surface plasmon resonance, they showed the binding of HRG to the extracellular domain of CLEC1A. They also demonstrated that a CLEC1A mAb inhibited the effects of native HRG on neutrophils and vascular endothelial cells (35). Similar inhibition by anti-CLEC1A mAb or anti-CLEC1A polyclonal Ab of HRG-induced bacterial phagocytosis observed in the current study strongly suggested the involvement of CLEC1A in the bacterial phagocytosis-enhancing effect of HRG on neutrophils.

In light of neutrophil events that are induced by HRG/CLEC1A interaction, CLEC1A will inevitably trigger crucial signal transductions to link the neutrophil events upon HRG binding. However, a downstream signal for CLEC1A has been surprisingly unknown (41), and for that reason, we could not specify and monitor the key signal molecules that will be activated in response to HRG binding to CLEC1A. To approach this point, another CLEC family protein like CLEC1B whose nature is well studied even in the signal transduction machinery may help to predict the unidentified CLEC1A signals. As shown in Fig. 8A, CLEC1B owns hemi-ITAM (HemITAM) in its N-terminal cytoplasmic tail, which recruits spleen-associated tyrosine kinase (SYK) when the Tyr^{7} in the hemITAM is phosphorylated, leading a CLEC1B-featured signal transduction with phosphorylation of several signal molecules that is appended on the exerted signal cascade. In contrast, we found the presence of one tyrosine (Tyr^{5}) through the entire cytoplasmic tail of CLEC1A, but the surrounding sequence of that tyrosine could not fit the reported tyrosine-based signaling motifs, which include not only HemITAM but also additional important motifs, such as the ITAMs and the ITIMs, the immunoreceptor tyrosine-switch motif (ITSM), the Ig tail tyrosine (ITT) motif, and an ITT-like motif (42). In addition, our Web-based motif searching unfortunately resulted in the presence of no appreciable sign of signaling motifs other than the tyrosine-based motifs through the entire sequence of the cytoplasmic region of CLEC1A. The signal transduction induced by CLEC1A stimulation remains to be determined (41). Facing the problem, in this study, we first tried to study whether HRG stimulates phosphorylation modification via CLEC1A. The approach brought about important information for

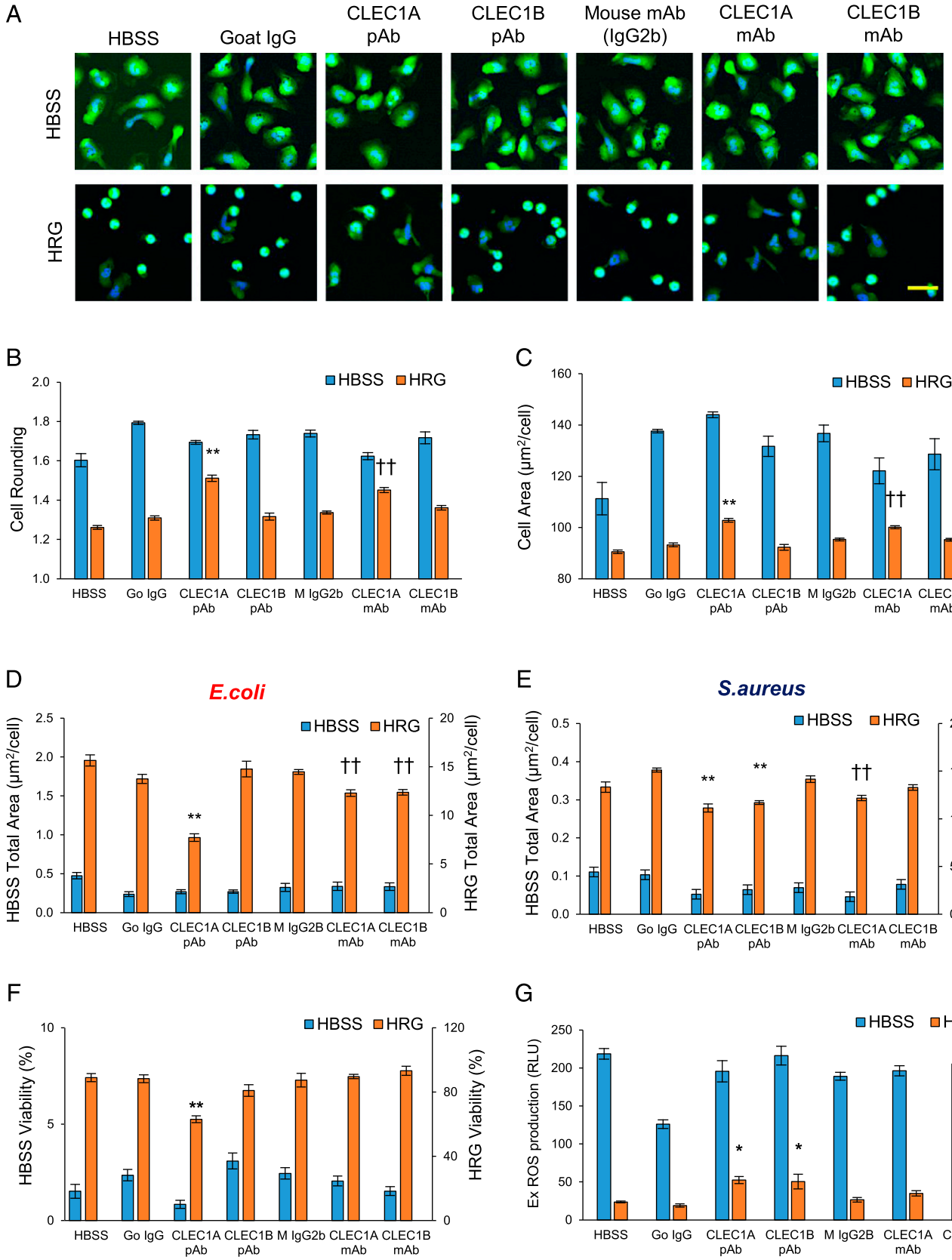

FIGURE 6. Receptor characterization for the effects of HRG on human neutrophils by blocking Abs. The experiments were performed by adding the appropriate CLEC Ab (goat control IgG, CLEC1A polyAb, CLEC1B polyAb, mouse IgG2b control Ab, CLEC1A mAb, and CLEC1B mAb: 10 μg/ml) to each assay. (**A**) The neutrophils were incubated in the presence or absence of HRG (0.25 μM). Different anti-CLEC Abs and control Abs were added to the incubation mixture at the start of incubation. The neutrophil shapes were determined at 60 min. The panel shows the results of labeling with Hoechst 33342 (blue) and calcein (green). Original magnification ×20 and digital zoom ×64; scale bar, 25 μm. (**B** and **C**) Bar graphs represent the cell area (μm²/cell) and cell rounding (average of maximum diameter/minimum diameter per cell) obtained from the neutrophil shape assay. $^{**}p < 0.01$ versus goat IgG pAb, $^{\dagger\dagger}p < 0.01$ versus mouse IgG2b mAb. (**D** and **E**) Bar graphs represent the HRG (0.25 μM)-induced neutrophil phagocytic activity against *E. coli* and *S. aureus* determined by the total phagocytic area in the presence of each Ab. $^{**}p < 0.01$ versus goat IgG pAb, $^{\dagger\dagger}p < 0.01$ versus mouse IgG2b mAb. (**F**) Bar graphs represent *(Figure legend continues)*

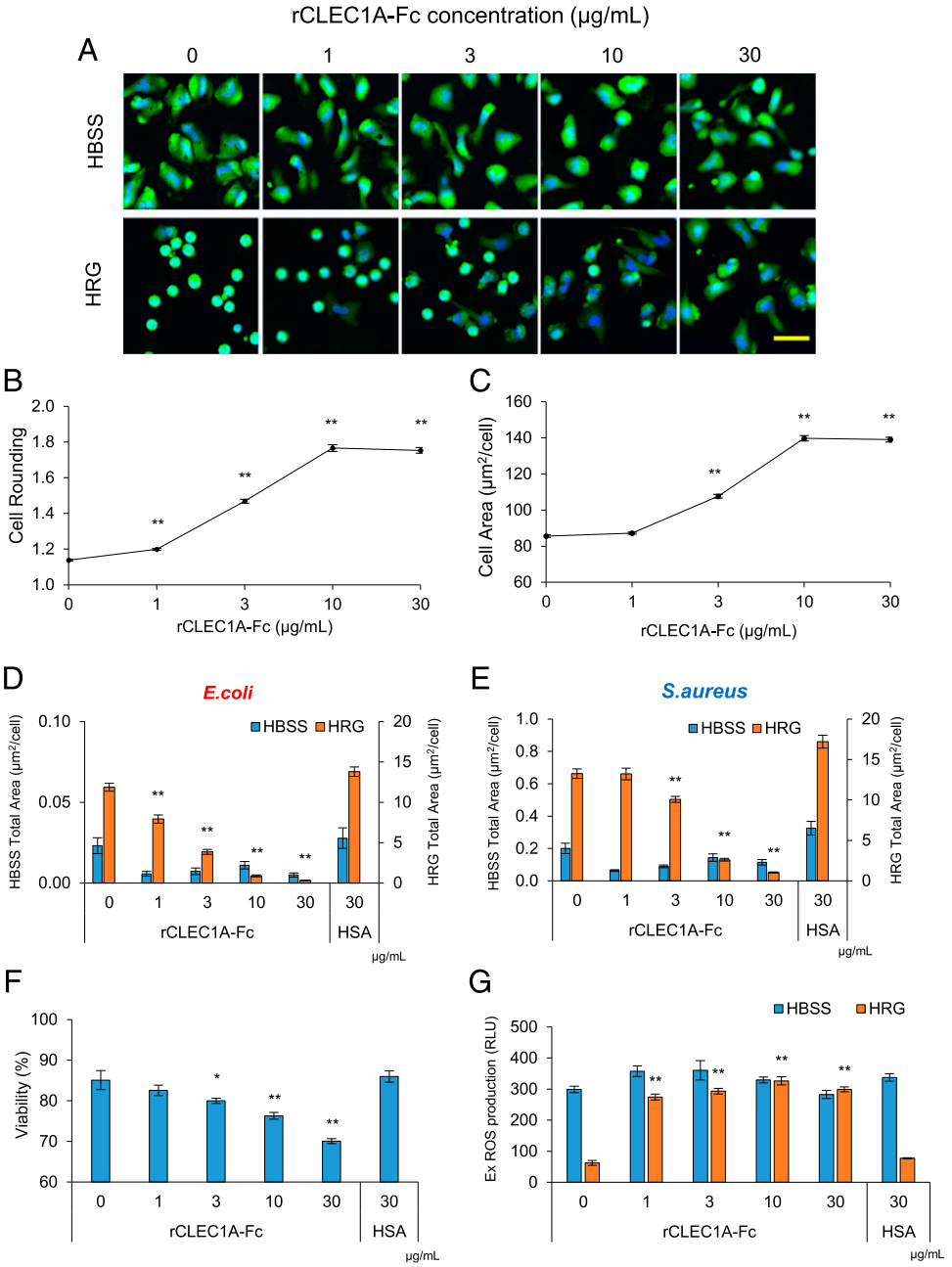

FIGURE 7. Morphological and functional regulation of human neutrophils by HRG were neutralized by the addition of rCLEC1A-Fc. The experiments were performed by adding the control protein (HSA 30 μg/ml) and rCLEC1A-Fc fusion protein (1–30 μg/ml) to each assay. (**A**) Results of the neutrophil shape assay with the control protein and rCLEC1A-Fc fusion protein in the presence or absence of HRG (0.25 μM). The panel shows the results of labeling with Hoechst 33342 (blue) and calcein (green). Original magnification ×20 and digital zoom ×64; scale bar, 25 μm. (**B** and **C**) Bar graphs represent the cell area (μm^2/cell) and cell rounding (average of maximum diameter/minimum diameter per cell) obtained from the neutrophil shape assay with the control protein and rCLEC1A-Fc fusion protein. $^{**}p < 0.01$ versus rCLEC1A-Fc 0 μg/m. (**D** and **E**) Bar graphs represent the total area obtained from neutrophil phagocytosis analysis with the control protein and rCLEC1A-Fc fusion protein in the presence of HRG (0.25 μM), *E. coli*, and *S. aureus*, respectively. $^{**}p < 0.01$ versus rCLEC1A-Fc 0 μg/m. (**F**) Bar graphs represent the viability (with the number of neutrophils at 0 h taken as 100%) obtained from the neutrophil viability assay with the control protein and rCLEC1A-Fc fusion protein in the presence of HRG (0.25 μM). $^{*}p < 0.05$, $^{**}p < 0.01$ versus rCLEC1A-Fc 0 μg/m. (**G**) Bar graphs represent the chemiluminescence (extracellular ROS production of neutrophils) obtained from the detections of neutrophil extracellular ROS production assay with the control protein and rCLEC1A-Fc fusion protein in the presence of HRG (0.25 μM). $^{**}p < 0.01$ versus rCLEC1A-Fc 0 μg/m. The results shown are the means ± SEM of 12 fields (B–F) or three wells (G).

the unidentified CLEC1A signaling; that is, phosphorylation of many proteins was highly induced by CLEC1A overexpression without HRG (Fig. 8B). Of our interest, the phosphorylation of the bands was further upregulated in part in response to the HRG treatment of the cells. These results suggest that HRG-CLEC1A owns its natured signal pathway(s) coupled with phosphorylation

neutrophil viability 24 h after the incubation with HRG (0.25 μM) in the presence of each Ab. $^{**}p < 0.01$ versus goat IgG pAb. (**G**) Bar graphs represent the extracellular ROS production of neutrophils in the presence of HRG (0.25 μM). Each Ab was added to the incubation mixture at the start of incubation, and the extracellular ROS level was determined at 30 min. $^{*}p < 0.05$ versus goat IgG pAb. The results shown are the means ± SEM of 12 fields (B–F) or three wells (G).

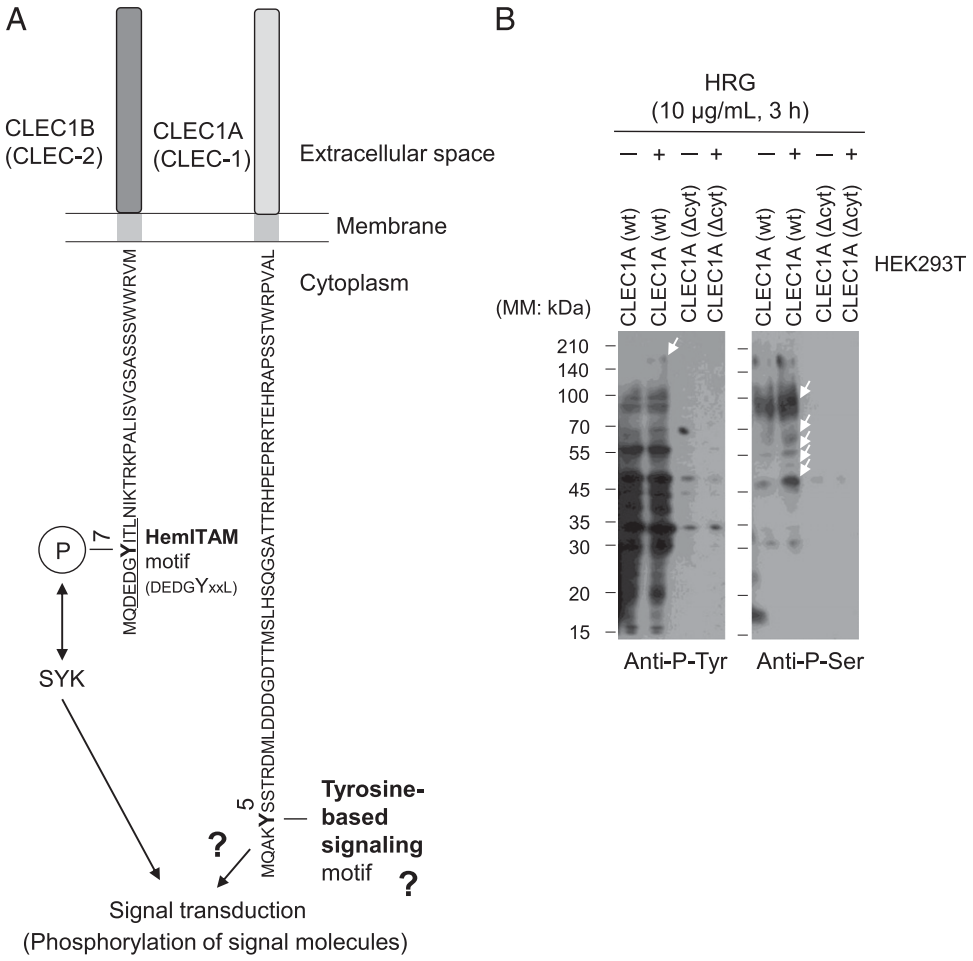

FIGURE 8. Detection of intracellular signals induced by HRG using CLEC1A-expressing HEK293T cells. (**A**) A diagram of signal transductions triggered by the cytoplasmic tails of CLEC1B and CLEC1A. (**B**) Western blotting data of the phosphorylated proteins in cells. The stable transformants originated in HEK293T cells that were expressing either CLEC1A (wt) or CLEC1A (cyt) in a sustained manner were treated or not treated with HRG recombinant protein at final concentration of 10 μg/ml for 3 h in cultures. After collecting the cell pellets, the pellets were lysed, loaded on SDS-PAGE, electrophoresed to separate the proteins according to their m.w., and transferred to the PVDF membrane. Phospho-proteins on the membrane were detected by using anti-phosphotyrosine (P-Tyr) Ab or anti-phosphoserine (P-Ser) Ab. Arrows show the upregulated proteins for their phosphorylation modification in response to the HRG treatment.

modification, which may contribute to the several neutrophil events. To unveil the HRG/CLEC1A axis–mediated signal cascade, identification of the phospho-proteins indicated by arrows (Fig. 8B) is required so that the subject is now part of our ongoing studies.

In the current study, we found that the stimulation of neutrophils by *E. coli* and *S. aureus* significantly decreased the expression of CLEC1A protein, whereas those by HRG and TNF-α did not (Supplemental Fig. 1A, 1B). In the case of stimulation by *E. coli*, the decrease in CLEC1A protein was associated with the reduction of CLEC1A mRNA (Supplemental Fig. 1C, 1D). These results suggest the possible pathway(s) triggered by both *E. coli* and *S. aureus*, which regulate the expression of CLEC1A. Further works are necessary on this line. It is noteworthy that the CLEC1B-blocking mAb slightly antagonized the effect of HRG on *E. coli* phagocytosis because the activation of NK cells by HRG was reported to be mediated by CLEC1B (43). Thus, we cannot exclude the possibility that CLEC1B is an accompanying receptor molecule for CLEC1A stimulation. Further work is necessary along this line. In contrast to the full agonist-like activities of the rHRG and native HRG, the rHRG-Fc fusion protein showed a partial agonist-like activity with regard to the neutrophil rounding effect (Supplemental Fig. 2A, 2B). Moreover, the rHRG-Fc fusion protein had no stimulatory effect on bacterial phagocytosis and did not induce a reduction of ROS production (Supplemental Fig. 2C–E). These results may imply that the added Fc hindered adequate binding of HRG to CLEC1A, and there might be multiple states of HRG-receptor complex formation associated with different neutrophil functions.

Neutrophils migrate to inflammatory sites and play critical roles for host defense by phagocytosing and killing bacteria. Patients with neutropenic or leukocyte adhesion deficiency are at increased risk for bacterial infection. In contrast, neutrophil effector functions, such as release of ROS and NETs, have been shown to sometimes damage host tissues in several diseases, including sepsis, in which such functions are not regulated properly. Wenisch et al. (44) reported that neutrophil functions (phagocytosis, killing, and ROS production) were significantly diminished in septic patients. Therefore, the adequate control of neutrophil function may be a target for treatment of sepsis-associated organ damage. In the previous (45) and the present studies, we observed that the isolated human neutrophils suspended in a serum-free or HRG-free medium produced higher levels of extracellular ROS spontaneously when compared with the ROS production in the presence of HRG (Fig. 5C). The neutrophils in the absence of HRG also showed the delay of passage through artificial microcapillaries and required prolonged time to pass through the microcapillaries as compared with those suspended in HRG-containing medium (28). Therefore, it was speculated that the removal of HRG from the medium induced the uncontrolled activation of neutrophils even under the nonstimulated condition in vitro and that a physiological concentration of HRG (1 μM) constantly maintains a state of circulating neutrophils at the basal level. The results showing the phagocytosis-enhancing effect of HRG indicate that such a basal state is also preferable to phagocytotic activity of neutrophils.

In our previous study, the plasma HRG levels were decreased markedly in septic CLP mice and septic patients in the intensive care unit (46). Supplementary treatment of septic mice

with purified human HRG significantly inhibited intravascular immunothrombus formation starting from neutrophil adhesion to vascular walls in the lung vasculatures (28). Moreover, HRG exerts a protective role on human vascular endothelial cells from excessive activation and lesion in vitro (35, 47). These in vitro and in vivo effects of HRG as a whole strongly suggest that HRG may play a homeostatic role by inhibiting the unnecessary activation of both neutrophils and vascular endothelial cells and by keeping the basal state of these two types of cells. It is quite likely that the phagocytosis-enhancing effects of HRG observed in the current study should contribute to the antiseptic effects of supplementary therapy of CLP mice.

Acknowledgments

Human fresh-frozen plasma was kindly provided by the Japanese Red Cross Society.

Disclosures

The authors have no financial conflicts of interest.

References

1. Sheats, M. K. 2019. A comparative review of equine SIRS, sepsis, and neutrophils. *Front. Vet. Sci.* 6: 69.
2. Etzioni, A. 2010. Defects in the leukocyte adhesion cascade. *Clin. Rev. Allergy Immunol.* 38: 54–60.
3. Lefrançais, E., B. Mallavia, H. Zhuo, C. S. Calfee, and M. R. Looney. 2018. Maladaptive role of neutrophil extracellular traps in pathogen-induced lung injury. *JCI Insight* 3: e98178.
4. Vardon-Bounes, F., S. Ruiz, M.-P. Gratacap, C. Garcia, B. Payrastre, and V. Minville. 2019. Platelets are critical key players in sepsis. *Int. J. Mol. Sci.* 20: 3494.
5. Singer, M. 2014. The role of mitochondrial dysfunction in sepsis-induced multi-organ failure. *Virulence* 5: 66–72.
6. Poon, I. K. H., K. K. Patel, D. S. Davis, C. R. Parish, and M. D. Hulett. 2011. Histidine-rich glycoprotein: the Swiss army knife of mammalian plasma. *Blood* 117: 2093–2101.
7. Koide, T., D. Foster, S. Yoshitake, and E. W. Davie. 1986. Amino acid sequence of human histidine-rich glycoprotein derived from the nucleotide sequence of its cDNA. *Biochemistry* 25: 2220–2225.
8. Jones, A. L., M. D. Hulett, and C. R. Parish. 2005. Histidine-rich glycoprotein: a novel adaptor protein in plasma that modulates the immune, vascular and coagulation systems. *Immunol. Cell Biol.* 83: 106–118.
9. Saito, H., L. T. Goodnough, J. M. Boyle, and N. Heimburger. 1982. Reduced histidine-rich glycoprotein levels in plasma of patients with advanced liver cirrhosis. Possible implications for enhanced fibrinolysis. *Am. J. Med.* 73: 179–182.
10. Sia, D. Y., D. B. Rylatt, and C. R. Parish. 1982. Anti-self receptors. V. Properties of a mouse serum factor that blocks autorosetting receptors on lymphocytes. *Immunology* 45: 207–216.
11. Leung, L. L., P. C. Harpel, and R. L. Nachman. 1989. Platelet histidine-rich glycoprotein. *Methods Enzymol.* 169: 268–276.
12. Jones, A. L., M. D. Hulett, and C. R. Parish. 2004. Histidine-rich glycoprotein binds to cell-surface heparan sulfate via its N-terminal domain following Zn2+ chelation. *J. Biol. Chem.* 279: 30114–30122.
13. Leung, L. L. 1986. Interaction of histidine-rich glycoprotein with fibrinogen and fibrin. *J. Clin. Invest.* 77: 1305–1311.
14. Lijnen, H. R., M. Hoylaerts, and D. Collen. 1980. Isolation and characterization of a human plasma protein with affinity for the lysine binding sites in plasminogen. Role in the regulation of fibrinolysis and identification as histidine-rich glycoprotein. *J. Biol. Chem.* 255: 10214–10222.
15. Leung, L. L., R. L. Nachman, and P. C. Harpel. 1984. Complex formation of platelet thrombospondin with histidine-rich glycoprotein. *J. Clin. Invest.* 73: 5–12.
16. Manderson, G. A., M. Martin, P. Onnerfjord, T. Saxne, A. Schmidtchen, T. E. Mollnes, D. Heinegård, and A. M. Blom. 2009. Interactions of histidine-rich glycoprotein with immunoglobulins and proteins of the complement system. *Mol. Immunol.* 46: 3388–3398.
17. Gorgani, N. N., B. A. Smith, D. H. Kono, and A. N. Theofilopoulos. 2002. Histidine-rich glycoprotein binds to DNA and Fc γ RI and potentiates the ingestion of apoptotic cells by macrophages. *J. Immunol.* 169: 4745–4751.
18. Gorgani, N. N., J. G. Altin, and C. R. Parish. 1999. Histidine-rich glycoprotein regulates the binding of monomeric IgG and immune complexes to monocytes. *Int. Immunol.* 11: 1275–1282.
19. Chang, N. S., R. W. Leu, J. K. Anderson, and J. E. Mole. 1994. Role of N-terminal domain of histidine-rich glycoprotein in modulation of macrophage Fc γ receptor-mediated phagocytosis. *Immunology* 81: 296–302.
20. Gorgani, N. N., C. R. Parish, S. B. Easterbrook Smith, and J. G. Altin. 1997. Histidine-rich glycoprotein binds to human IgG and C1q and inhibits the formation of insoluble immune complexes. *Biochemistry* 36: 6653–6662.
21. Morgan, W. T. 1981. Interactions of the histidine-rich glycoprotein of serum with metals. *Biochemistry* 20: 1054–1061.
22. Katagiri, M., K. Tsutsui, T. Yamano, Y. Shimonishi, and F. Ishibashi. 1987. Interaction of heme with a synthetic peptide mimicking the putative heme-binding site of histidine-rich glycoprotein. *Biochem. Biophys. Res. Commun.* 149: 1070–1076.
23. Rydengård, V., O. Shannon, K. Lundqvist, L. Kacprzyk, A. Chalupka, A. K. Olsson, M. Mörgelin, W. Jahnen-Dechent, M. Malmsten, and A. Schmidtchen. 2008. Histidine-rich glycoprotein protects from systemic Candida infection. *PLoS Pathog.* 4: e1000116.
24. Shannon, O., V. Rydengård, A. Schmidtchen, M. Mörgelin, P. Alm, O. E. Sørensen, and L. Björck. 2010. Histidine-rich glycoprotein promotes bacterial entrapment in clots and decreases mortality in a mouse model of sepsis. *Blood* 116: 2365–2372.
25. Bosshart, H., and M. Heinzelmann. 2003. Endotoxin-neutralizing effects of histidine-rich peptides. *FEBS Lett.* 553: 135–140.
26. Poon, I. K. H., M. D. Hulett, and C. R. Parish. 2010. Histidine-rich glycoprotein is a novel plasma pattern recognition molecule that recruits IgG to facilitate necrotic cell clearance via FcgammaRI on phagocytes. *Blood* 115: 2473–2482.
27. Tsuchida-Straeten, N., S. Ensslen, C. Schäfer, M. Wöltje, B. Denecke, M. Moser, S. Gräber, S. Wakabayashi, T. Koide, and W. Jahnen-Dechent. 2005. Enhanced blood coagulation and fibrinolysis in mice lacking histidine-rich glycoprotein (HRG). *J. Thromb. Haemost.* 3: 865–872.
28. Wake, H., S. Mori, K. Liu, Y. Morioka, K. Teshigawara, M. Sakaguchi, K. Kuroda, Y. Gao, H. Takahashi, A. Ohtsuka, et al. 2016. Histidine-rich glycoprotein prevents septic lethality through regulation of immunothrombosis and inflammation. *EBioMedicine* 9: 180–194.
29. Plato, A., J. A. Willment, and G. D. Brown. 2013. C-type lectin-like receptors of the dectin-1 cluster: ligands and signaling pathways. *Int. Rev. Immunol.* 32: 134–156.
30. Sancho, D., and C. Reis e Sousa. 2012. Signaling by myeloid C-type lectin receptors in immunity and homeostasis. *Annu. Rev. Immunol.* 30: 491–529.
31. Huysamen, C., and G. D. Brown. 2009. The fungal pattern recognition receptor, Dectin-1, and the associated cluster of C-type lectin-like receptors. *FEMS Microbiol. Lett.* 290: 121–128.
32. Lopez Robles, M. D., A. Pallier, V. Huchet, L. L. Texier, S. Remy, C. Braudeau, L. Delbos, A. Moreau, C. Louvet, C. Brosseau, et al. 2017. Cell-surface C-type lectin-like receptor CLEC-1 dampens dendritic cell activation and downstream Th17 responses. *Blood Adv.* 1: 557–568.
33. Thebault, P., N. Lhermite, G. Tilly, L. Le Texier, T. Quillard, M. Heslan, I. Anegon, J. P. Soulillou, S. Brouard, B. Charreau, et al. 2009. The C-type lectin-like receptor CLEC-1, expressed by myeloid cells and endothelial cells, is up-regulated by immunoregulatory mediators and moderates T cell activation. *J. Immunol.* 183: 3099–3108.
34. Sattler, S., D. Reiche, C. Sturtzel, I. Karas, S. Richter, M. L. Kalb, W. Gregor, and E. Hofer. 2012. The human C-type lectin-like receptor CLEC-1 is upregulated by TGF-β and primarily localized in the endoplasmic membrane compartment. *Scand. J. Immunol.* 75: 282–292.
35. Shangze, G., H. Wake, M. Sakaguchi, D. Wang, Y. Takahashi, K. Teshigawara, H. Zhong, S. Mori, K. Liu, H. K. Takahashi, and M. Nishibori. 2020. Histidine-rich glycoprotein inhibits high-mobility group box-1-mediated pathways in vascular endothelial cells through CLEC-1A. *iScience* 23: 101180.
36. Sumardika, I. W., Y. Chen, N. Tomonobu, R. Kinoshita, I. M. W. Ruma, H. Sato, E. Kondo, Y. Inoue, A. Yamauchi, H. Murata, et al. 2019. Neuroplastin-β mediates S100A8/A9-induced lung cancer disseminative progression. *Mol. Carcinog.* 58: 980–995.
37. Chen, Y., I. W. Sumardika, N. Tomonobu, I. M. Winarsa Ruma, R. Kinoshita, E. Kondo, Y. Inoue, H. Sato, A. Yamauchi, H. Murata, et al. 2019. Melanoma cell adhesion molecule is the driving force behind the dissemination of melanoma upon S100A8/A9 binding in the original skin lesion. *Cancer Lett.* 452: 178–190.
38. Chen, Y., I. W. Sumardika, N. Tomonobu, R. Kinoshita, Y. Inoue, H. Iioka, Y. Mitsui, K. Saito, I. M. W. Ruma, H. Sato, et al. 2019. Critical role of the MCAM-ETV4 axis triggered by extracellular S100A8/A9 in breast cancer aggressiveness. *Neoplasia* 21: 627–640.
39. Mori, S., H. K. Takahashi, K. Yamaoka, M. Okamoto, and M. Nishibori. 2003. High affinity binding of serum histidine-rich glycoprotein to nickel-nitrilotriacetic acid: the application to microquantification. *Life Sci.* 73: 93–102.
40. Izquierdo, I., M. N. Barrachina, L. Hermida-Nogueira, V. Casas, L. A. Morán, S. Lacerenza, R. Pinto-Llorente, J. A. Eble, V. de Los Ríos, E. Domínguez, et al. 2020. A comprehensive tyrosine phosphoproteomic analysis reveals novel components of the platelet CLEC-2 signaling cascade. *Thromb. Haemost.* 120: 262–276.
41. Chiffoleau, E. 2018. C-Type lectin-like receptors as emerging orchestrators of sterile inflammation represent potential therapeutic targets. *Front. Immunol.* 9: 227.
42. Bauer, B., and A. Steinle. 2017. HemITAM: a single tyrosine motif that packs a punch. *Sci. Signal.* 10: eaan3676.
43. Nishimura, Y., H. Wake, K. Teshigawara, D. Wang, M. Sakaguchi, F. Otsuka, and M. Nishibori. 2019. Histidine-rich glycoprotein augments natural killer cell function by modulating PD-1 expression via CLEC-1B. *Pharmacol. Res. Perspect.* 7: e00481.

44. Wenisch, C., P. Fladerer, S. Patruta, R. Krause, and W. Hörl. 2001. Assessment of neutrophil function in patients with septic shock: comparison of methods. *Clin. Diagn. Lab. Immunol.* 8: 178–180.
45. Htwe, S. S., H. Wake, K. Liu, K. Teshigawara, B. S. Stonestreet, Y.-P. Lim, and M. Nishibori. 2018. Inter-α inhibitor proteins maintain neutrophils in a resting state by regulating shape and reducing ROS production. *Blood Adv.* 2: 1923–1934.
46. Kuroda, K., H. Wake, S. Mori, S. Hinotsu, M. Nishibori, and H. Morimatsu. 2018. Decrease in histidine-rich glycoprotein as a novel biomarker to predict sepsis among systemic inflammatory response syndrome. *Crit. Care Med.* 46: 570–576.
47. Gao, S., H. Wake, Y. Gao, D. Wang, S. Mori, K. Liu, K. Teshigawara, H. Takahashi, and M. Nishibori. 2019. Histidine-rich glycoprotein ameliorates endothelial barrier dysfunction through regulation of NF-κB and MAPK signal pathway. *Br. J. Pharmacol.* 176: 2808–2824.